Understanding Phonon Transmission in $SrTiO_3/PbTiO_3$ Superlattices Using Atomistic Green's Function

Isaac Perez*
Department of Materials Science and Engineering, Cornell University, Ithaca, NY 14850
(Dated: August 18, 2025)

$SrTiO_3/PbTiO_3$ (STO/PTO) superlattices have been previously studied for their unique topological phases due to their strong coupling between polarization and strain. These properties, particularly heat conductivity, can be tuned by varying the thickness of layers, the strain imposed by the substrate, and the application of an external electric field, making them a strong candidate for novel energy harvesting, phononic storage, and computation devices. The atomistic Green's function method (AGF) has emerged as a valuable tool for understanding phonon transport across interfaces. The document below outlines how I may apply AGF to understand the heat-conducting properties of STO/PTO superlattices and their evolution under the influence of an external electric field using first-principle calculations and molecular dynamics (MD) using machine learning potentials.

I. BACKGROUND

Superlattices have become objects of deep interest due to their tunable material properties, particularly heat conductivity. For example, researchers were able to measure the change in thermal conductivity in strain symmetrized Si/Ge superlattices on Si(111) [1]. Furthermore, ferroelectric materials were not only found to have a tunable thermal conductivity via experimentally accessible fields [2], but the domain walls (DWs) can be *written* and *erased*, providing a versatile way to dynamically modulate heat fluxes [3]. The combination of these properties makes STO/PTO superlattices great candidates for the creation of efficient heat management, energy harvesting, and phononic computation and storage devices.

Modeling these systems has been met with difficulties as large supercells are required to model DWs, hampering the use of accurate *ab initio* methods such as density-functional theory (DFT). Furthermore, the relatively poor transferability and accuracy of the interatomic potential modes available for perovskite oxides have limited the use of molecular dynamics to model these larger systems . However, the use of machine learning interatomic potentials offers versatile and transferable potentials [4], potentially circumventing the latter problem.

To understand the nature of thermal conductivity in superlattices, particularly how heat is transferred at the interfaces, I use AGF methods. AGF methods allow for the calculation of a transmission probability function, giving us information about which vibrational modes are transmitted through the interface. With a little more work, I am able to find the polarization-specific transmission functions. Note that this is not possible with the standard AGF output and requires additional mode-resolved analysis rather than being a trivial extension of the method. While the transmission probability function gives us a lot of valuable information, I can use it to calculate the heat conductivity of the superlattice. It is important to note that the two most common atomistic transport models besides AGF are direct MD methods and lattice dynamics (LD). MD is the most direct of these three methods, simulating the thermal properties in the time domain. Direct MD methods were not used here as spectral phonon transmission information requires the use of carefully controlled MD simulations known as wave packet simulations, typically involving specific initial displacement patterns. Furthermore, direct MD methods are expected to be used at temperatures higher than the Debye temperature, where the quantum nature of phonon occupation can be ignored.

Furthermore, AGF considers the lattice-dynamical equations and, unlike LD, requires only a few matrices that embed in the contacts; detailed boundary conditions are handled through the self-energies, making the method most compatible with standard density functional perturbation theory (DFPT)/MD workflows. The AGF method is ideally suited for a geometry shown in Fig. 1, where a small "device" region is connected by large reservoirs, also called contacts, that are held at constant temperature. AGF methods aim to compute the spectral transmissivity for phonon transport from contact 1 to contact 2 to obtain the interface thermal conductance. It's important to note that the device is assumed to be small enough that phonon transport can be considered ballistic or coherent. This is not much of an issue to begin with as wave-like phonons dominate the heat-conducting properties of superlattices when the layer thickness is kept small but more advanced formulations can include anharmonic phonon-phonon scattering, which captures incoherent transport beyond the harmonic AGF framework.

To calculate the thermal properties at the interface, AGF must first calculate the transmission probability function with respect to angular frequency, given as

$$\mathcal{T}(\omega) = \mathrm{Tr}[\Gamma_L G_d \Gamma_R G_d^\dagger] \tag{1}$$

* iperez@hmc.edu

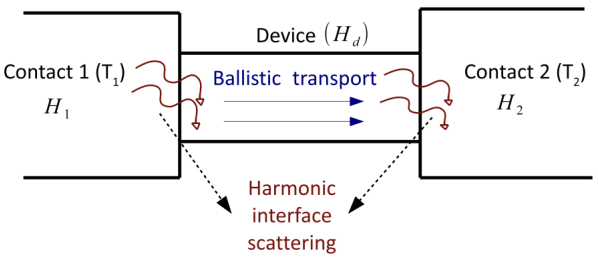

FIG. 1. Schematic of a typical phonon transport problem considered by AGF formulation. It is assumed that all reflections and mode mixing due to harmonic scattering are encoded at the boundary and coherent phonon transport occurs in the device region. H_1, H_2 and H_d represent the harmonic matrices of isolated contacts and the device, respectively. [5]

Where G_d represents the subset of the total Green's function corresponding to the device and Γ_L and Γ_R is the "escape rate" or "braodening matrices" for the connection between the left (or right) contact at the device, given as

$$\Gamma_{L(R)} = i[\Sigma_{L(R)} - \Sigma^{\dagger}_{L(R)}]$$

where Σ is the self-energy matrix associated with either the left or right contact. Using the transmission probability function and Landauer expressions [6], the heat current is given as

$$J = \frac{1}{2\pi}\int_0^{\infty} \hbar\omega\mathcal{T}(\omega)[n_B(\omega, T_L) - n_B(\omega, T_R)]d\omega$$

where n_B is the Bose-Einstein distribution and the linear response thermal conductance for small ΔT is given as,

$$\kappa(T) = \frac{1}{2\pi}\int_0^{\infty} \hbar\omega\mathcal{T}(\omega)\frac{\partial n_B(\omega, T)}{\partial T}d\omega \qquad (2)$$

II. METHODS

A. AGF Implementation

The AGF method was implemented in Python and began with the loading of the interatomic force constants (IFCs) of the system, calculated using Abinit and loaded using Abipy. Since we are isolating the interface in the device, the contacts are modeled as bulk STO and PTO, respectively. Loading the IFCs and atomic masses allows us to construct the mass-normalized dynamical matrices, whose components are given by

$$H_{ij} = \frac{\Phi_{ij}}{\sqrt{m_i m_j}}$$

where Φ_{ij} are the force constants and m_i is the atomic mass. From bulk STO and PTO IFCs, we can extract the onsite force constants within a layer, H_{00}, and interlayer coupling constants to the next layer, H_{01}. These are required to compute the surface Green's functions for the semi-infinite contacts. From the 1x1 superlattice IFCs, we then build the full device dynamical matrix H_C using only the interactions within the central region.

The program will then identify the atoms at the edges of the STO and PTO bulk structures and the left and right sides of the superlattice cell. This allows us to calculate the portion of the mass-normalized dynamical matrices associated with the coupling between the semi-infinite contacts and the finite device.

$$H_{CL} = \text{coupling between STO and superlattice}$$
$$H_{CR} = \text{coupling between PTO and superlattice}$$

I then compute the retarded surface Green's function of each semi-infinite contact using the Sancho–Rubio decimation ("doubling") scheme, which iteratively integrates out deeper layers of the lead along the transport direction. First, atoms are grouped into principal layers, the smallest repeatable unit such that the lead dynamical matrix is block-tridiagonal, with on-site block H_{00} and nearest-layer couplings H_{01} and $H_{10} = H_{01}^{\dagger}$. Defining $z = (\omega + i0^+)^2$ with a small $0^+ > 0$ (we use $0^+ = 10^{-4}$ in code), the iteration starts from

$$\begin{aligned} \varepsilon^{(0)} &= H_{00} \\ \alpha^{(0)} &= H_{01} \\ \beta^{(0)} &= H_{10} \\ g^{(n)} &= \left[zI - \varepsilon^{(n)}\right]^{-1} \end{aligned}$$

and renormalizes the surface layer as

$$\begin{aligned} \varepsilon^{(n+1)} &= \varepsilon^{(n)} + \alpha^{(n)} g^{(n)} \beta^{(n)} + \beta^{(n)} g^{(n)} \alpha^{(n)} \\ \alpha^{(n+1)} &= \alpha^{(n)} g^{(n)} \alpha^{(n)} \\ \beta^{(n+1)} &= \beta^{(n)} g^{(n)} \beta^{(n)}. \end{aligned}$$

When the couplings vanish numerically (we use a tolerance of 10^{-8}), the surface Green's function is $g_s(\omega) = \left[zI - \varepsilon^{(n_\star)}\right]^{-1}$. These $g_L(\omega)$ and $g_R(\omega)$ are then embedded into the device via the self-energies

$$\begin{aligned} \Sigma_{L(R)}(\omega) &= H^{\dagger}_{C\,L(R)}\, g_{L(R)}(\omega)\, H_{C\,L(R)} \\ \Gamma_{L(R)} &= i\Big(\Sigma_{L(R)} - \Sigma^{\dagger}_{L(R)}\Big), \end{aligned}$$

so that the device Green's function and transmission are

$$\begin{aligned} G_C(\omega) &= \left[zI - H_C - \Sigma_L - \Sigma_R\right]^{-1} \\ \mathcal{T}(\omega) &= \mathrm{Tr}\Big[\Gamma_L G_C \Gamma_R G_C^{\dagger}\Big]. \end{aligned}$$

This lets us compute $\mathcal{T}(\omega)$ on a frequency grid using only the bulk IFC-derived blocks (H_{00}, H_{01}) for each contact, the device matrix H_C, and the interface couplings

$H_{C\,L}, H_{C\,R}$, while the semi-infinite parts of the leads are accounted for through g_s.

It is essential to note that the factor 0^+ is a damping factor associated with connecting our finite system to the hypothetical infinite bulk in the contacts. As long as 0^+ is smaller than the characteristic frequency resolution, results are unaffected apart from an artificial broadening of sharp modes. Prior literature suggests,

$$0^+(\omega) = \delta_0 \omega^2 \qquad \delta_0 \in (10^{-9}, 10^{-3})$$

As the value of δ_0 is reduced, accuracy improves as computational cost increases.

B. Computational Details

To calculate the IFCs of bulk STO and PTO, I used the popular DFT software Abinit, which uses DFPT. In all calculations, I used the norm-conserving pseudopotentials obtained from the PseudoDojo database constructed using the Perdew-Burke-Ernzerhof (PBE) GGA exchange-correlation functional. The IFCs of bulk STO were calculated using a 6x6x6 Monkhorst-Pack k/q point grid with an ecut of 50 Ha and a 6x6x6 Monkhorst-Pack k/q point grid with an ecut of 40 Ha for PTO. As for the 1x1 STO/PTO superlattice cell, I used a cubic cell with a relaxed lattice parameter 3.6133602807 Å and calculated IFCs using a 6x6x6 Monkhorst-Pack k/q point grid and an ecut of 40 Ha. The stress induced on the lattice was given as,

$$\text{stress tensor}\Big[\text{GPa}\Big] = \begin{pmatrix} -7.4875 & 0.0 & 0.0 \\ 0.0 & -7.4875 & 0.0 \\ 0.0 & 0.0 & 14.9839 \end{pmatrix}$$

after relaxation under constraints. As stated previously, I set 0^+ to be 10^{-4} and converged the surface Green's function with a tolerance set to 10^{-8}. In the future, I would like to have the factor δ_0 be dependent on the frequency of the mode ω.

C. Experimental Setup

To give us insight into the effect of external electric fields on STO/PTO superlattices, the largest challenge to overcome is the simulation of DWs, as DWs often require extensive cells, too large for first-principle calculations to handle. As stated previously, the best way to circumvent this problem is to use MD, a less computationally intensive way to calculate the large cells required to simulate DWs. As ground truth, I've chosen to simulate the unperturbed 1x1 superlattice cell using DFT. This calculation will be reproduced using MD to ensure that the ML potentials that will be used in the MD simulation are representative of our first-principles calculations. Furthermore, to capture longer-range effects that are present in the periodic superlattice, I will extend the device to include more than a single interface. The biggest issue when doing this is that the phonons must stay coherent in the harmonic formulation of the AGF method. While I expect wave-like phonons to dominate for superlattices with single alternating layers, as the mean free path of the phonon will be larger than the spacing between interfaces, it will be important for me to consider the effect of anharmonic extensions of the AGF method. I expect that the results will converge as I continue to add layers to the device. This will also open up the possibility of simulating 2x2, 2x3, 3x2, and 3x3 lattices, although these will be more difficult to simulate using first-principle calculations. Furthermore, I would like to do a quick study to understand how my results change if I were to manually freeze in DWs in the device, a crude approximation of DWs, which will hopefully capture their qualitative features. It would be convenient if a rough approximation of the DWs captured the behavior observed in a more realistic simulation of the DWs in STO/PTO superlattices.

Using the above first-principle calculations, I can then help train my ML potentials that will be used in MD simulations. Using LAMMPS, I plan to rerun many of the first-principle calculations run above to ensure that my ML potentials accurately represent the interatomic potentials calculated in the first-principle calculations. Once I ensure this is the case, I will use MD to extend the size of my cells, particularly when freezing in the DWs. With this series of calculations, I hope to gain a better understanding of the effect of the external electric field (and therefore DWs) on the thermal properties of the lattice. If we can gain a deeper understanding of how the phonon modes are being filtered by the DWs and layer thickness, we can hopefully be in a much more informed position to predict materials with similar properties as STO/PTO superlattices.

III. FUTURE WORK

Moving forward, I hope to continue the calculations outlined above. As of the end of my stay at PARADIM at Cornell University, I was able to finish the calculation for the IFCs of bulk STO, PTO, and STO/PTO 1x1 superlattice. While I've also become more familiar with MD, particularly LAMMPS, while at PARADIM, I would still like to continue learning how to effectively use the software and use ML potentials. I will also need to do more research on which ML potential I would like to move forward with; there is a plethora for me to try.

Finally, I would like to note that most of my time at PARADIM was spent growing STO/PTO superlattices and developing software for this project that, while it was not ultimately used in the final version of this project, will be repurposed for other projects being conducted at Harvey Mudd College.

IV. ACKNOWLEDGMENTS

I would like to thank the PARADIM Thin Film and Theory & Simulation Facilities at Cornell University for giving me the resources to grow these STO/PTO superlattices while conducting this research. I would also like to thank my mentors, Dylan Sotir and Drake Niedzielski, for their support, and Harvey Mudd College for this opportunity.

[1] S. Chakraborty, C. A. Kleint, A. Heinrich, C. M. Schneider, J. Schumann, M. Falke, and S. Teichert, enThermal conductivity in strain symmetrized Si/Ge superlattices on Si(111), Applied Physics Letters **83**, 4184 (2003).

[2] J. A. Seijas-Bellido, H. Aramberri, J. Íñiguez, and R. Rurali, enElectric control of the heat flux through electrophononic effects, Physical Review B **97**, 184306 (2018).

[3] J. A. Seijas-Bellido, C. Escorihuela-Sayalero, M. Royo, M. P. Ljungberg, J. C. Wojdeł, J. Íñiguez, and R. Rurali, enA phononic switch based on ferroelectric domain walls, Physical Review B **96**, 140101 (2017).

[4] G. Wang, C. Wang, X. Zhang, Z. Li, J. Zhou, and Z. Sun, enMachine learning interatomic potential: Bridge the gap between small-scale models and realistic device-scale simulations, iScience **27**, 109673 (2024).

[5] S. Sadasivam, Y. Che, Z. Huang, L. Chen, S. Kumar, and T. S. Fisher, enTHE ATOMISTIC GREEN'S FUNCTION METHOD FOR INTERFACIAL PHONON TRANSPORT, Annual Review of Heat Transfer **17**, 89 (2014).

[6] S. G. Das and A. Dhar, enLandauer formula for phonon heat conduction: relation between energy transmittance and transmission coefficient (2012), arXiv:1204.5595 [cond-mat].